Journal of Catalysis 272 (2010) 320–332

Contents lists available at ScienceDirect

Journal of Catalysis

journal homepage: www.elsevier.com/locate/jcat

Theoretical study on the structure–reactivity relationships of acetylacetone–Fe catalyst modified by ionic compound in C–H activation reaction

Xingbang Hu [a,b], Yong Sun [a], Jianyong Mao [a], Haoran Li [a,*]

[a] Department of Chemistry, Zhejiang University, Hangzhou 310027, PR China
[b] School of Chemistry and Chemical Engineering, Nanjing University, Nanjing 210093, PR China

ARTICLE INFO

Article history:
Received 25 February 2010
Revised 21 April 2010
Accepted 23 April 2010
Available online 21 May 2010

Keywords:
Structure–reactivity relationship
C–H activation
Acetylacetone–Fe
Anion
Cation
Methane
Ionic compound

ABSTRACT

The reactivity of acetylacetone–Fe can be tuned by introducing an ionic compound (IC) group onto the ligand in the investigation into 41 different catalysts. This IC-modification alters the spin density carried by Fe/O atoms (SD_{Fe}/SD_O), the charge carried by O atom (Q_O), and the isotropic fermi contact couplings of O atom ($IFCC_O$) in the Fe=O part, thereby influencing the reactivity of the catalyst. The IC-modification that increases the SD_O, Q_O, and $IFCC_O$ or decreases the SD_{Fe} can make the catalyst more powerful. The order of the correlation between the structure parameters and reactivity is $SD_O > Q_O > SD_{Fe} \approx IFCC_O > LUMO_C–HOMO_R \gg LUMO_C–HOMO_C \approx Q_{Fe}$. Changing the anion of the IC-catalyst is a more effective way to increase the reactivity compared with changing the cation, and the order is $PF_6^- > AlCl_4^- > BF_4^- > AsF_6^- > SbF_6^- > AlF_4^- > CF_3CO_2^- > CF_3SO_3^- > NO_3^- > Cl^-$. Long distance between the IC part and the catalytic active center however weakens the influence induced by the IC-modification. These structure–reactivity relationships are expected to be used in catalyst design.

1. Introduction

Homogeneous catalysts offer their own distinct advantages; however, they are not easily recovered. Developing water-soluble catalyst is an effective way for recycling it [1,2]. Modifying the catalysts by ionic compound (IC) (including ionic liquid) is a recent development in this field [3,4]. These catalysts modified by IC are easily retrieved and recycled because their solubility can be adjusted by using different cation–anion combinations, enabling phase separation from less polar organic solvents to aqueous media. For examples, IC-modified ruthenium carbene can be reused 10 times in ring-closing metathesis [5,6], IC-modified salen-Mn catalysts can be reused 10 times without any losing of reactivity for the enantioselective epoxidation of styrene [7], IC-modified diphenylphosphine palladium can be reused at least six times for the Suzuki–Miyaura reaction [8], and so on. Because the expensive or poisonous catalysts can be recovered by IC-modification, many similar methods have been developed [3–24].

Though it has been well known that IC-modification can change catalyst solubility [3–24], it is still unclear how exactly it influences their catalytic ability. Some studies suggested that IC-modification improved the catalyst reactivity [7,18–24]. In the asymmetric addition of trimethylsilyl cyanide to benzaldehyde, for example, the catalytic turnover frequency (TOF) values for chiral vanadyl salen catalysts modified by IC, silica, single-wall carbon nanotubes, and activated carbon were 18.3, 2.7, 3.1, and 3.8 h^{-1} respectively, indicating that IC-modification makes the catalyst a most powerful one [18]. A research on CO_2 and epoxide copolymerization showed that salen-cobalt catalyst could be greatly activated by IC-modification [19]. In the asymmetric aldol reaction, the IC-modified proline was found to be more effective than the normal proline [20]. In another asymmetric aldol reaction, the IC-modified cis-4-hydroxy-l-proline showed quite high TOF (up to 930) [21]. The IC-modified salen-Mn catalysts were also found to be more powerful than the unmodified one [7,22]. Imidazolium-based Fe-containing IC was found to be more effective than the normal $FeCl_2$ catalyst for the dimerization of bicyclo [2.2.1] hepta-2,5-diene [23]. Recently, we developed an IC-modified acetylacetone–Fe, and this catalyst also showed higher reactivity for oxidation reaction than its unmodified counterpart [24]. Some studies also suggested that IC-modification depressed the reactivity. The asymmetric transfer-hydrogenation of acetophenone catalyzed by conventional ruthenium catalyst gave a conversion rate of 95% in 24 h, whereas the conversion rate of the same reaction catalyzed by modified ruthenium catalyst was only 80% in 24 h [9]. Besides these, there was no comparison on the reactivity between the IC-modified catalysts and their unmodified counterpart in other reported Refs. [11–17].

All of these experiments indicated that the influences of the IC-modification on the catalytic ability were quite complicated. It will be helpful in understanding the origin of the catalyst reactivity if

* Corresponding author. Fax: +86 571 8795 1895.
E-mail address: lihr@zju.edu.cn (H. Li).

0021-9517/$ - see front matter © 2010 Elsevier Inc. All rights reserved.
doi:10.1016/j.jcat.2010.04.016

the structure–reactivity relationship can be established. Many theoretic researches (including molecular dynamics simulations and quantum chemistry calculations) have been performed to investigate the property of the IC [25–28]. However, most of these researches focused mainly on the structure characters of the IC and the interaction between the ions and the solvents. As far as we know, there are few theoretic works about the structure character and reactivity of the catalysts modified by IC. We believe that the reactivity of the IC-modified catalysts is governed by different cation–anion combinations. However, what position should the IC group be connected? To what extent does the IC-modification influence the reactivity? Which one is more powerful to alter the catalytic ability, anion or cation? Furthermore, what is the order of different anions and cations? There are so many questions in designing IC-modified catalyst.

We chose methane oxidation, regarded as a touchstone reaction of catalytic reactivity, to test the catalysts. While many inorganic [29–34] and metal-organic [35–39] catalysts have been reported for the activation of methane, better understanding on the roles of IC-modification is sure to be helpful in improving the reactivity of existing methane oxidation catalysts.

2. Computational methods

This study generated many optimized structures which can be found in the Supplementary material.

The B3LYP method, widely used in methane oxidation catalyzed by metal-organic catalysts [35–39], has also been used with satisfying results in IC systems [27,28]. For this reason, we optimized all the structures by the B3LYP method. In the methane oxidation catalyzed by the metal-organic catalysts, 6-31G basis set was generally used for these atoms except transition metal [36,37,40]. It was necessary to take the relativistic effect of the transition metal and heavy element into consideration [35–40]. In this manuscript, five different basis sets were used (basis set A: LANL2DZ for Fe/As/Sb and 6-31G for the other atoms; basis set B: CEP-121G for Fe/As/Sb and 6-31G* for the other atoms; basis set C: CEP-121G for Fe/As/Sb and 6-311+G* for the other atoms; basis set D: LANL2DZ for Fe/As/Sb and 6-311++G** for the other atoms; and basis set E: CEP-121G for Fe/As/Sb and 6-311++G** for the other atoms. Basis set A was used unless otherwise mentioned). Geometric configuration optimization, energy calculation, frequency calculation, zero-point energy correction, and natural bond orbital (NBO) analysis were performed by using the same basis set. The effect of basis set superposition error (BSSE) has been analyzed by means of the counterpoise correction method.

Transition metal catalysts are known to have low-spin state (LSS) and high-spin state (HSS) [41], both of which were investigated in this study. For the specific catalyst investigated, the LSS means that there are two isolated electrons in the system (the spin multiplicity is 3), and the HSS means that there are four (the spin multiplicity is 5).

The computed stationary points have been characterized as minima or transition states by diagonalizing the Hessian matrix and analyzing the vibrational normal modes. In this way, the stationary points can be classified as minima if no imaginary frequencies are shown or as transition states if only one imaginary frequency is obtained. The particular nature of the transition states has been determined by analyzing the motion described by the eigenvector associated with the imaginary frequency. The reaction pathway was confirmed by intrinsic reaction coordinate (IRC) analysis.

To estimate the effects of the environment, a PCM single point energy calculation using the polarizable conductor calculation model (CPCM) was performed on the optimized structure in gas phase. The solvents used here covered the following dielectric constants: $\varepsilon = 4.9$, 8.9, 20.7, 36.6, and 78.4. All calculations were performed with the Gaussian 03 suite of programs [42].

3. Results and discussion

The acetylacetone–Fe is a metal-organic catalyst widely used for the oxidation, polymerization, and some other reactions [43–45]. Catalysts based on acetylacetone–metal are cheap and easy to be synthesized. However, it is difficult to recover this catalyst from the organic solution by water wash method, due to its bad solubility in water and good solubility in organic solvent. IC-modification can make the catalyst reusable. Recently, we had synthesized a simple and reusable IC-modified acetylacetone–Fe catalyst by a two-step reaction. Furthermore, it showed higher catalytic ability for oxidation reaction compared with the traditional acetylacetone–Fe [24].

To further improve the performance of acetylacetone–Fe (or similar catalysts) requires a better understanding on the structure–reactivity relationship. In this manuscript, we investigated a series of acetylacetone–Fe catalysts modified by IC (IC-catalyst) and its unmodified counterpart (NIC-catalyst) (Fig. 1). Totally 41 different catalysts were investigated, including 9 IC-catalysts with different cations (ammonium, pyridinium, and imidazolium salts), 10 IC-catalysts with different anions, 7 NIC-catalysts, and 8 catalysts with pyridine as axial ligand (LSS and HSS). The IC-catalysts with different cations are abbreviated as [IC-*n*][Cl] ($n = 1$–9), the IC-catalysts with different anions are abbreviated as [IC-1][X] (X = BF_4, PF_6, SbF_6, AsF_6, CF_3SO_3, CF_3CO_2, NO_3, AlF_4, $AlCl_4$, and Cl), the NIC-catalysts are abbreviated as NIC-*n* ($n = 1$–7), and the catalysts with pyridine as axial ligand are abbreviated as [IC-*n*][X]-py or NIC-*n*-py. NIC-4 and NIC-7 are two special NIC-catalysts because the acid (HF and HCl) forms hydrogen bond with the catalysts.

3.1. The structural changes of catalyst induced by the IC-modification

Because the LSS reaction pathway is more energy favorable (demonstrated in Sections 3.2 and 3.4), the LSS catalysts are used unless otherwise mentioned.

Some representative structural parameters of the optimized catalysts were listed in Table 1. For the IC-catalysts, the negative charges carried by the anion range from −0.453 to −0.794. This value obviously depends on the variety of cation and anion. The minimum distances between the anion and cation change from 1.639 to 2.336 Å. These values are typical for the IC [25–28] and indicate the ionic character of the modified catalysts.

The Fe=O part is the active center of both the IC- and NIC-catalysts. The Fe–O bond length ranges from 1.630 to 1.634 Å for different IC- and NIC-catalysts. These are closed to the same value of Compound I of P450 catalyst (B3LYP method, basis set used: LACVP for Fe and the 6-31G for the rest of the atoms) [37], POM-Fe=O catalyst (B3LYP method, basis set used: LANL2DZ) [46] and (N_4Py)Fe=O catalyst (B3LYP method, basis set used: LACVP for Fe and the 6-31G for the rest of the atoms) [47]. At the same time, the spin density and charge carried by the Fe and O atom of NIC- and IC-catalysts are also reasonable comparing with above three organic-metal catalysts containing Fe=O active center.

The IC-modification has a remarkable effect on the Fe=O part, especially on the SD and *Q* values carried by the Fe and O atoms. Interestingly, some relationships among part of the parameters can be found (Fig. 2). Taking the SD_{Fe} as example, it ranges from 1.129 to 1.151 for IC-catalysts with different anion and from 1.179 to 1.223 for NIC-catalysts. The SD_{Fe} of all IC-catalysts with different anions is smaller than these of NIC-catalysts. For NIC-catalysts, the SD_{Fe} is reduced when it forms hydrogen bond with acid

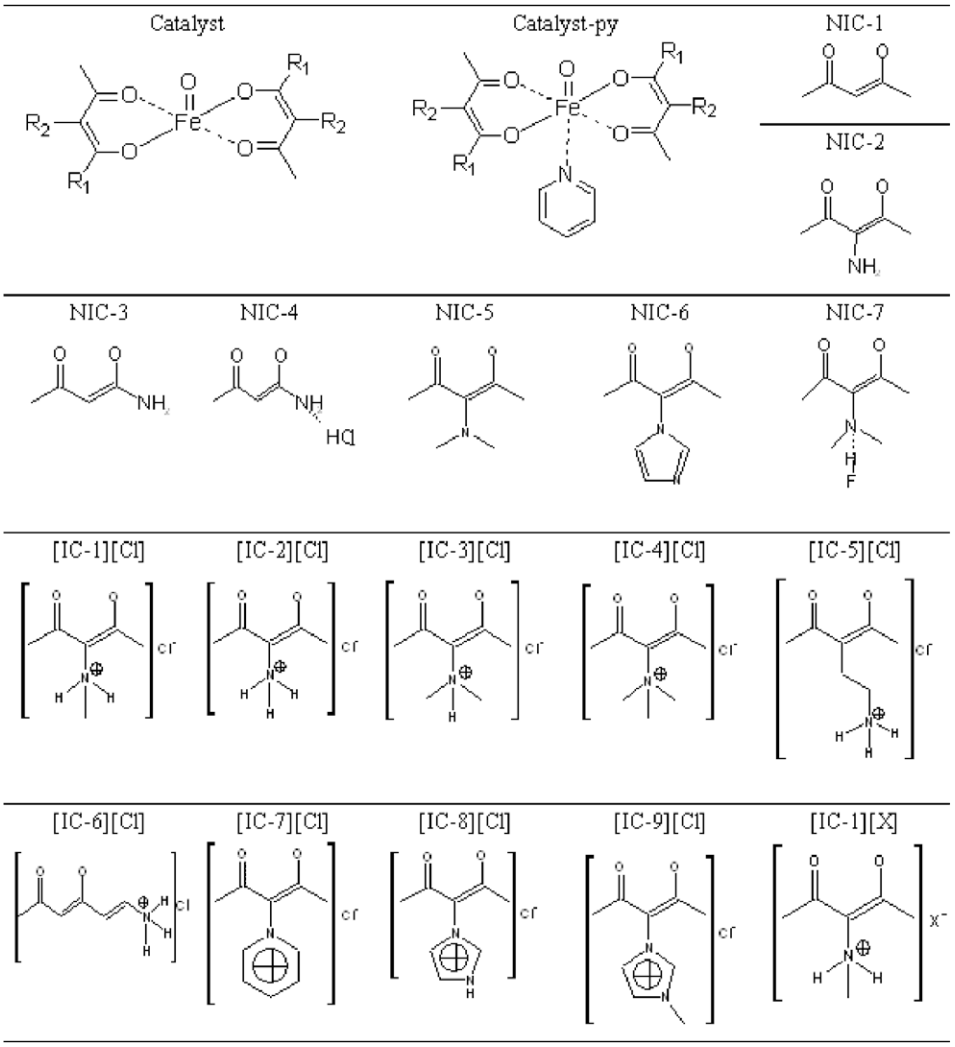

Fig. 1. Structures of the NIC- and IC-catalyst with different cations and anions. The main structure of the catalyst was shown in the catalyst column. The other columns show the variety of R_1 and R_2 group. X = BF_4, PF_6, SbF_6, AsF_6, CF_3SO_3, CF_3CO_2, NO_3, AlF_4, and $AlCl_4$.

(The discrepancy between the SD_{Fe} of NIC-3 and NIC-4 is 0.037). Excluding these NIC-catalysts with hydrogen bond (NIC-4 and NIC-7), the SD_{Fe} of NIC-catalysts is 1.193–1.223. For the IC-catalysts with different cation, the SD_{Fe} is 1.148–1.194. It has intersection with the NIC-catalysts, indicating that some of the IC-modification methods have only slight influence on the electric structure of the active center. [IC-5][Cl] is a typical example. The IC part and the active center of [IC-5][Cl] are connected by $–CH_2CH_2–$ group, hence the electric influence of IC-modification on Fe=O active center is not strong. Therefore, the SD_{Fe} of [IC-5][Cl] is quite close to some of the NIC-catalysts (It can be found that [IC-5][Cl] also shows similar reactivity to some of the NIC-catalysts in Section 3.3). Sometimes, the purpose of IC-modification is to change only the solubility but not the reactivity [11–17]. In this case, the IC part should be kept away from the catalytic active center, and these two parts should be connected with single bond. Many previous researches have adopted such modification methods [3,4]. For example, the experimental results have shown that the tetrafluoroborate imidazolium only slightly improved the reactivity of the salen-Mn catalyst when it connects with the salen-Mn by $–CH_2NHCH_2CH_2CH_2–$ group [7].

The SD_O of the Fe=O part are also well regulated. The SD_O of all IC-catalysts with different anions are larger than those of the NIC-catalyst. For the charge carried by Fe and O atoms, no rule can be found in Q_{Fe} values, whereas Q_O show similar rule to the SD_{Fe} (Fig. 2 and Table 1). It is worth noticing that the O atoms of most IC-catalysts carry less negative charge compared with that of NIC-catalyst, especially for the O atoms of the [IC-1][X] catalysts. It suggests an unnegligible electron transfer occurring from O to Fe atom during the IC-modification.

IC-modification has also remarkable influence on the IFCC of O atoms. The $IFCC_O$ shows similar trend to the SD_O and Q_O. Though IC-modification can change the gap between the HOMO and LUMO of the catalyst, no rule can be found out (Fig. 2).

Based on above results and discussion, it can be found that a remarkable electron transfer occurs from O to Fe atom during the IC-modification for most of the IC-catalysts. There are some relationships among part of the parameters (such as SD_{Fe}, SD_O, Q_O, or $IFCC_O$). In an effort to find out the structure–reactivity relationship, we investigated the IC- and NIC-catalysts in methane oxidation.

3.2. Methane oxidation catalyzed by IC- and NIC-catalysts

In this manuscript, the whole reaction processes catalyzed by NIC-1-py, [IC-1][Cl]-py, NIC-1, and [IC-1][Cl] were investigated. For the other catalysts, only the rate-determining step was investigated. The reactant, transition state, intermediate, and product in the reaction catalyzed by IC-catalyst are henceforth abbreviated

Table 1
Structure parameters of different catalysts.

	r(Fe–O)[a]	r(a–c)[b]	SD_{Fe}	SD_O	Q_{Fe}	Q_O	Q_{anion}[c]	$IFCC_O$ (a.u.)	Gap[d]
[IC-1][Cl]	1.631	1.747	1.158	0.859	0.695	−0.301	−0.564	0.1407	0.0016
[IC-2][Cl]	1.631	1.655	1.148	0.868	0.692	−0.294	−0.499	0.1418	0.0023
[IC-3][Cl]	1.631	1.851	1.183	0.835	0.707	−0.323	−0.615	0.1387	0.0024
[IC-4][Cl]	1.631	2.336	1.149	0.855	0.742	−0.295	−0.732	0.1385	0.0223
[IC-5][Cl]	1.633	1.761	1.194	0.822	0.700	−0.327	−0.587	0.1363	0.0011
[IC-6][Cl]	1.632	1.700	1.187	0.830	0.714	−0.321	−0.550	0.1375	0.0112
[IC-7][Cl]	1.632	2.312	1.193	0.827	0.690	−0.324	−0.453	0.1373	0.0015
[IC-8][Cl]	1.631	1.695	1.171	0.849	0.694	−0.307	−0.586	0.1396	0.0021
[IC-9][Cl]	1.633	2.024	1.193	0.823	0.700	−0.328	−0.716	0.1370	0.0196
[IC-1][BF_4]	1.630	1.684	1.142	0.876	0.693	−0.286	−0.758	0.1420	0.3963
[IC-1][AlF_4]	1.630	1.639	1.148	0.870	0.697	−0.291	−0.737	0.1415	0.4071
[IC-1][$AlCl_4$]	1.630	2.228	1.139	0.879	0.702	−0.284	−0.794	0.1425	0.0011
[IC-1][PF_6]	1.630	1.742	1.129	0.888	0.696	−0.276	−0.786	0.1431	0.3729
[IC-1][AsF_6]	1.630	1.730	1.132	0.885	0.694	−0.278	−0.780	0.1429	0.3453
[IC-1][SbF_6]	1.630	1.719	1.135	0.882	0.693	−0.280	−0.765	0.1427	0.4245
[IC-1][CF_3SO_3]	1.630	1.671	1.147	0.870	0.683	−0.290	−0.745	0.1414	0.1708
[IC-1][CF_3CO_2]	1.631	1.645	1.151	0.867	0.690	−0.293	−0.707	0.1411	0.1333
[IC-1][NO_3]	1.630	1.740	1.149	0.868	0.691	−0.291	−0.708	0.1412	0.0041
NIC-1	1.633		1.203	0.815	0.700	−0.334		0.1361	0.4694
NIC-2	1.635		1.223	0.798	0.685	−0.351		0.1347	0.2484
NIC-3	1.632		1.216	0.793	0.712	−0.344		0.1334	0.3450
NIC-4	1.631		1.179	0.832	0.716	−0.318		0.1376	0.3891
NIC-5	1.634		1.218	0.803	0.680	−0.345		0.1349	0.0629
NIC-6	1.632		1.193	0.827	0.689	−0.325		0.1373	0.0007
NIC-7	1.633		1.193	0.825	0.689	−0.329		0.1372	0.3893

[a] Distance between Fe and O (in Å).
[b] The minimum distance between the anion and cation (in Å).
[c] The charge carried by anion.
[d] The HOMO–LUMO gap of the catalyst (in eV).

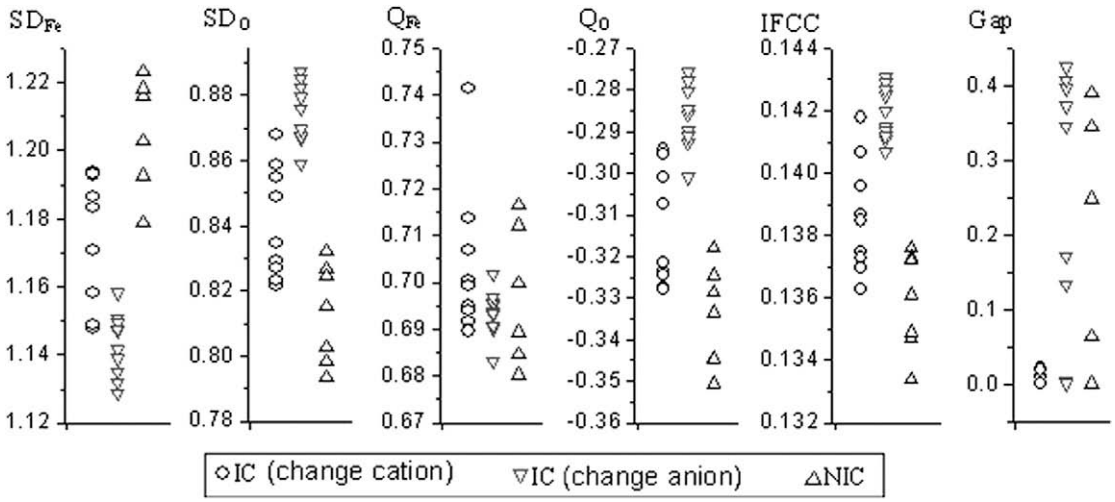

Fig. 2. The variation of the structure parameter induced by the IC-modifications.

as $^{3(5)}$IC-Rea, $^{3(5)}$IC-TS, $^{3(5)}$IC-Int, and $^{3(5)}$IC-Pro respectively (superscript values on the left denote spin multiplicities). Similarly, they are abbreviated as $^{3(5)}$NIC-Rea, $^{3(5)}$NIC-TS, $^{3(5)}$NIC-Int, and $^{3(5)}$NIC-Pro in the reaction catalyzed by NIC-catalyst.

Two different methane approaching methods were taken into consideration: method A, CH_4 approaches the catalyst from the direction as shown in Fig. 3; method B, CH_4 approaches from the aliphatic groups of the catalyst (Fig. S1 in Supplementary material). It was found that methane approaching the catalysts by method A gave higher binding energy than that by method B (Table 2). Furthermore, the optimized transition states of method B are the same to those of method A (Fig. S1). Hence, we focused mainly on the reactions with CH_4 approaching the catalysts by method A.

In this reaction, CH_4 interacts with the Fe=O part through a weak Fe=O···H–CH_3 interaction. The SD value carried by the reactant CH_4 is almost zero, indicating that almost no electron transfer occurs between CH_4 and the catalyst during the establishment of the Fe=O···H–CH_3 interaction. Methane oxidation catalyzed by Fe=O compounds (e.g. porphyrin–Fe [36,37] or all-metal–Fe complex [33,34]) generally includes the C–H activation and C–O rebound steps, both of which were investigated here. A series of electron transfer processes accompany the methane oxidation catalyzed by both the NIC-1-py and [IC-1][Cl]-py catalysts. The electron transfer processes and the geometric configuration changes are similar for the reaction catalyzed by both of the catalysts (Fig. 3 and Table 3). This indicates that this modification does not change the intrinsic reaction pathway. However, it was found that IC-modification did significantly change the energy barriers of the C–H activation and C–O rebound processes.

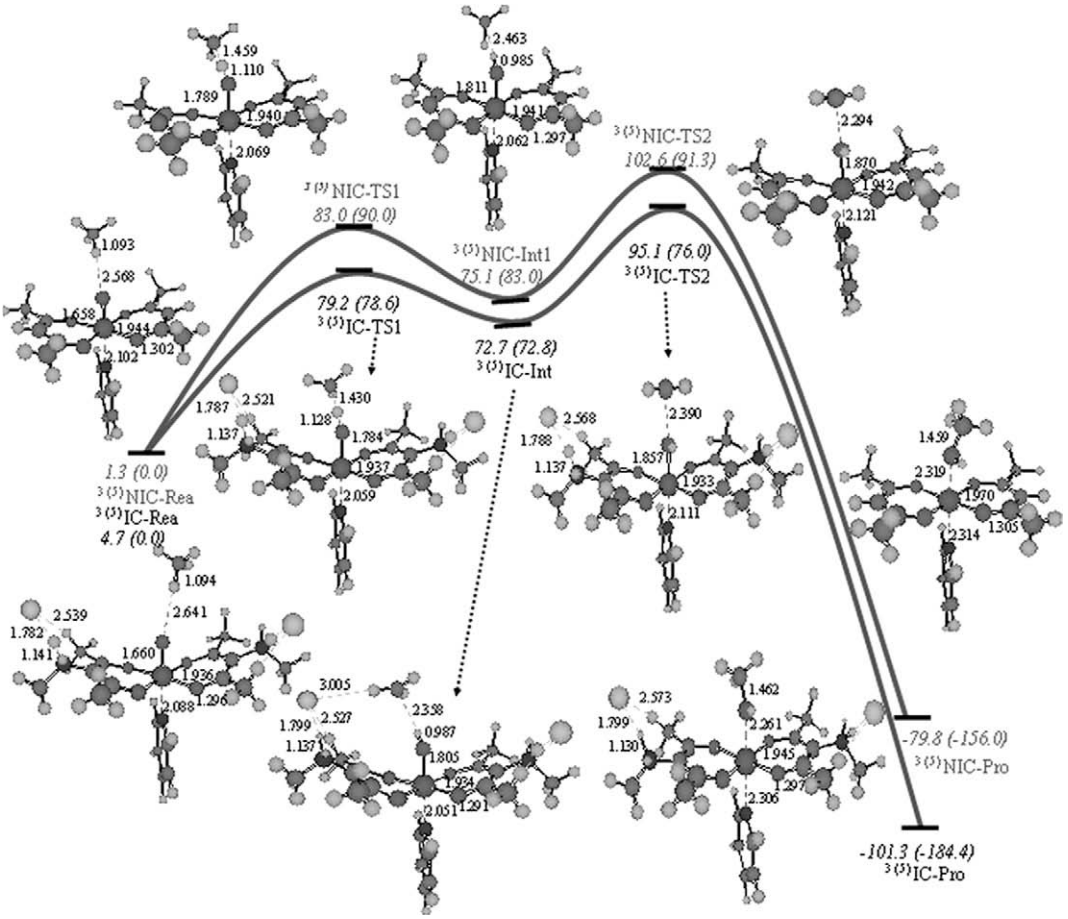

Fig. 3. The energy diagram of methane oxidation catalyzed by the [IC-1][Cl]-py and NIC-1-py catalysts. Values in italic denote relative enthalpy change in kJ/mol. The other values denote bond lengths in Å. Values out (in) parentheses are those for the low (high)-spin state.

Table 2
The binding energy (in kJ/mol) between the catalysts and methane.[a]

	Method A[b]	Method B[c]
NIC-1		
LSS	−2.7 (−2.6)	0.1 (0.0)
HSS	−2.1 (−2.0)	
[IC-1][Cl]-py		
LSS	−1.5 (−1.3)	−1.7 (−1.2)
HSS	−0.1 (0.1)	

[a] Values in the parentheses include BSSE correction.
[b] Methane approaching from the direction as shown in Fig. 3.
[c] Methane approaching from the aliphatic groups of the catalyst as shown in Fig. S1.

Table 3
The spin densities of the reactant, transition states, intermediate, and product.[a]

	Rea	TS1	Int	TS2	Pro
NIC-1-py					
Fe	1.08 (3.02)	0.90 (2.80)	0.90 (2.81)	1.28 (2.97)	2.00 (3.75)
O	0.98 (0.68)	0.53 (0.36)	0.16 (0.01)	−0.07 (−0.12)	0.02 (0.02)
CH_3	0.00 (0.00)	0.67 (0.67)	0.97 (0.96)	0.81 (0.92)	0.01 (0.00)
H[b]	0.00 (0.00)	−0.07 (−0.06)	0.00 (0.01)	0.01 (0.01)	0.00 (0.00)
[IC-1][Cl]-py					
Fe	1.03 (2.98)	0.87 (2.80)	0.88 (2.80)	1.25 (3.02)	2.00 (3.75)
O	1.02 (0.73)	0.57 (0.39)	0.19 (0.03)	−0.05 (−0.14)	0.02 (0.02)
CH_3	0.00 (0.00)	0.67 (0.64)	0.96 (0.94)	0.83 (0.89)	0.01 (0.00)
H[b]	0.00 (0.00)	−0.06 (−0.04)	0.00 (0.01)	0.01 (0.01)	0.00 (0.00)

[a] Values in parentheses denote the HSS.
[b] The transferred hydrogen.

(1) C–H activation step: one hydrogen in CH_4 transfers to the Fe=O part via a transition state TS1. The TS1 carries a negative SD value on the migrating hydrogen (Table 3), as it is typical for hydrogen abstraction processes by radicals [33,36,37]. The spin densities on Fe/O and CH_4 change significantly during the transition from Rea to TS1, indicating that the C–H activation step is a proton coupling with electron transfer process. In the LSS, the energy barrier is 81.7 kJ/mol for C–H activation catalyzed by the NIC-1-py and only 74.5 kJ/mol for that catalyzed by the [IC-1][Cl]-py catalyst. In the HSS, this barrier is 90.0 kJ/mol with NIC-1-py and 78.6 kJ/mol with [IC-1][Cl]-py as catalyst. Two results can be obtained: the [IC-1][Cl]-py is more powerful and the LSS reaction path is more energy favorable.

(2) C–O rebound step: after the C–H activation, the methyl group moves toward the oxygen atom via another transition state TS2. The energy barriers of the C–O rebound step are 27.5 and 8.3 kJ/mol for the LSS and HSS respectively when catalyzed by the NIC-1-py. The same figures are 22.4 and 3.2 kJ/mol when catalyzed by the [IC-1][Cl]-py. The C–O rebound process produces the final product CH_3OH. From NIC-Rea to NIC-Pro, the net energy changes are −81.1 and −156.0 kJ/mol respectively for the LSS and HSS. From IC-Rea to IC-Pro, the same values are −106.0 and −184.4 kJ/mol.

When there is no axial ligand, the most favorable sites for the anion (Cl^-) binding are still the one shown in Fig. 3 (Fig. S2 in Supplementary material) due to the strong anion–cation interaction. The reaction processes catalyzed by NIC-1 and [IC-1][Cl] show similar characters to these catalyzed by NIC-1-py and [IC-1][Cl]-py (Fig. 4). The biggest difference is that the pyridine as axial ligand can reduce the reaction barrier [37,39,40]. Hence, the C–H activation barrier catalyzed by NIC-1 is higher than that catalyzed by NIC-1-py. Similarly, the barrier catalyzed by [IC-1][Cl] is higher than that catalyzed by [IC-1][Cl]-py. Besides these, other characters are not influenced by the pyridine axial ligand, such as C–H activation step being the rate-determining step and [IC-1][Cl] being more powerful than NIC-1. Because some of the IC-modified catalysts reported here are complicated and taking pyridine into consideration will further add the burden of the computers, we focused mainly on the rate-determining step catalyzed by NIC-*n* (*n* = 1–7) and [IC-*n*][X] (*n* = 1–9, X = BF_4, PF_6, SbF_6, AsF_6, CF_3SO_3, CF_3CO_2, NO_3, AlF_4, $AlCl_4$ and Cl) in Section 3.3.

3.3. The structure–reactivity relationship of the IC- and NIC-catalysts without axial ligand

The rate-determining step (C–H activation step) catalyzed by 18 IC-catalysts and 7 NIC-catalysts was investigated in this section, and the structure parameters of these catalysts were correlated with their reactivities in this section.

3.3.1. The reactivity of IC- and NIC-catalysts

NIC-2, NIC-3, and NIC-5 catalysts are traditional acetylacetone–Fe (NIC-1) modified by amine. The C–H activation barriers catalyzed by NIC-2, NIC-3, and NIC-5 are quite close to that catalyzed by NIC-1 (Fig. 5). NIC-4 is NIC-3 forming hydrogen bond with HCl and NIC-7 is a HF hydrogen bond compound. Forming hydrogen bond can reduce the barrier by 5.2 and 4.9 kJ/mol for NIC-4 and NIC-7, respectively. NIC-6 is NIC-1 modified by imidazole. The C–H activation barrier catalyzed by NIC-6 is 6.3 kJ/mol lower than that catalyzed by NIC-1.

[IC-2][Cl], [IC-3][Cl], and [IC-4][Cl] are analogs to [IC-1][Cl]. The cation center N atoms of these catalysts connect with different number of H atoms or methyl groups. The anion (Cl^-) interacts with these H atoms or methyl groups by hydrogen bond (Fig. 6). Comparing [IC-2][Cl] with [IC-1][Cl], it can be found that replacing the methyl by hydrogen lowers the barrier by 2.2 kJ/mol. Similarly, replacing the hydrogen on the N atom of [IC-1][Cl] by methyl increases the barrier by 1.9 kJ/mol ([IC-1][Cl] vs [IC-3][Cl]). For [IC-5][Cl], the R1 group is $-CH_2CH_2-[NH_3][Cl]$. The ionic part ($[NH_3][Cl]$) indirectly connects with the active center (Fe=O) of the catalyst. Therefore, the influence induced by the ionic modification is weakened. The modification of $[NH_3][Cl]$ lowers the barrier by 11.8 kJ/mol in [IC-2][Cl], whereas it only reduces the barrier by 4.9 kJ/mol in [IC-5][Cl]. The influence induced by the pyridinium and imidazolium salts is weaker than that by the ammonium salts. The barriers catalyzed by [IC-7][Cl], [IC-8][Cl], and [IC-9][Cl] are higher than those catalyzed by [IC-1][Cl], [IC-2][Cl], and [IC-4][Cl]. However, they are still more powerful than the unmodified catalyst NIC-1.

Totally 10 different anions are used in this manuscript: BF_4^-, PF_6^-, SbF_6^-, AsF_6^-, $CF_3SO_3^-$, $CF_3CO_2^-$, NO_3^-, AlF_4^-, $AlCl_4^-$, and Cl^-. The reactivity of the catalysts is strongly affected by the counterion and follows the order: $PF_6^- > AlCl_4^- > BF_4^- > AsF_6^- > SbF_6^- > AlF_4^- > CF_3CO_2^- > CF_3SO_3^- > NO_3^- > Cl^-$ (Fig. 7). Catalyst with PF_6^- as anion has the most powerful reactivity. In the asymmetric hydrogenation of unfunctionalized olefins with cationic iridium–PHOX catalysts, BF_4^-, PF_6^-, and $CF_3SO_3^-$ have been used as the counterions. The experimental results revealed that the reactivity of the catalysts is $PF_6^- > BF_4^- > CF_3SO_3^-$, which shows the same order to our calculated results [48]. Besides, in the addition of arylboronic acids to aldehydes, catalyst with PF_6^- anion also shows more powerful reactivity than catalyst with BF_4^- anion [49].

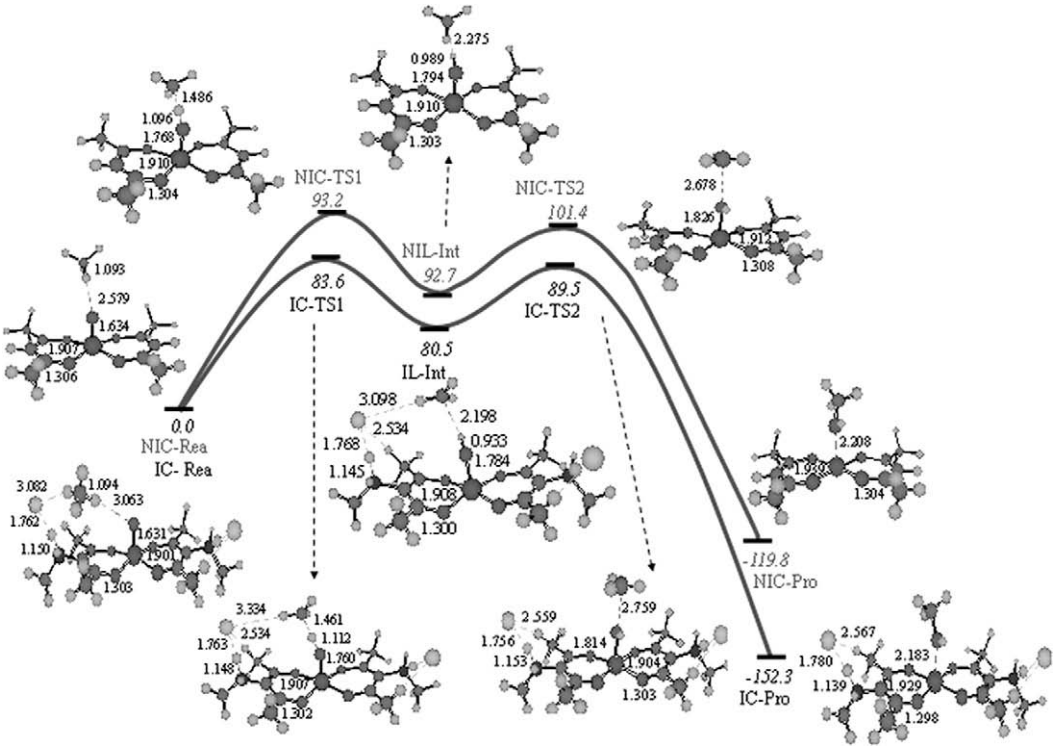

Fig. 4. The energy diagram of methane oxidation catalyzed by the [IC-1][Cl] and NIC-1 catalysts. Values in italic denote relative enthalpy change in kJ/mol for LSS. The other values denote bond lengths in Å.

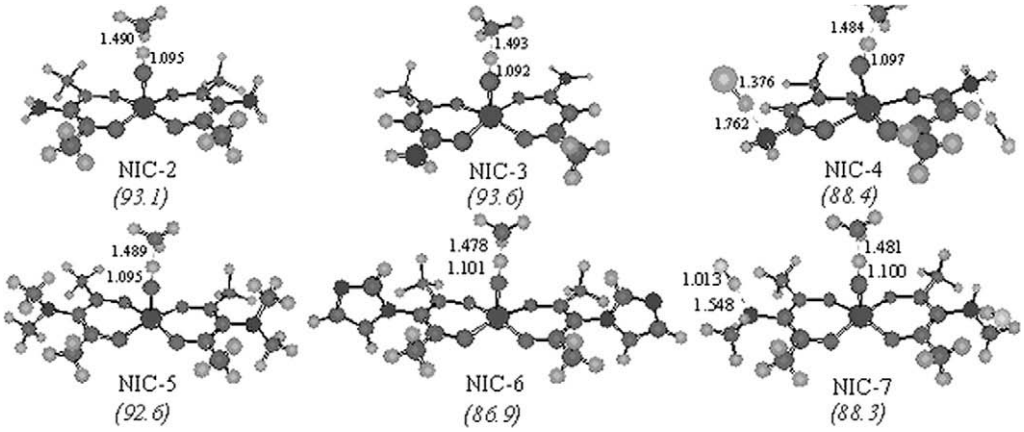

Fig. 5. The optimized transition states catalyzed by different NIC-catalysts. The values in parenthesis mean reaction barrier in kJ/mol. The other values denote bond lengths in Å.

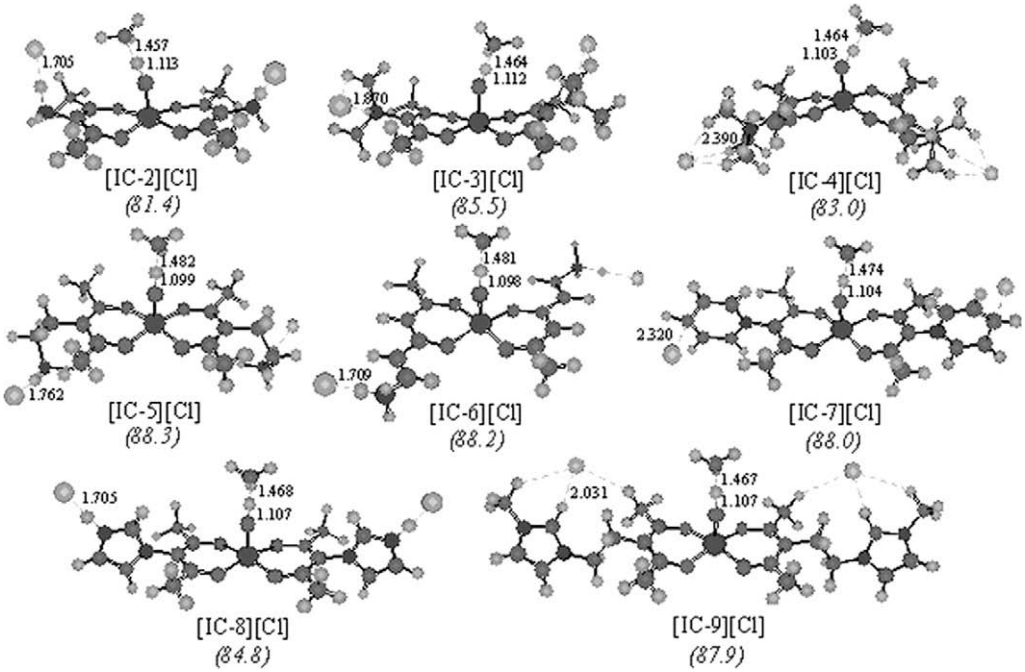

Fig. 6. The optimized transition states catalyzed by IC-catalyst with different cations. The values in parenthesis mean reaction barrier in kJ/mol. The other values denote bond lengths in Å.

Totally nine different cations were tested, and the barrier ranges from 81.4 to 88.3 kJ/mol. The lowest value is 81.4 kJ/mol. Ten different anions were investigated, and the barrier ranges from 74.7 to 83.6 kJ/mol. The lowest value is 74.7 kJ/mol. It seems that the anion is more powerful to increase the reactivity of the IC-catalyst than the cation. Fortunately, changing anion is easier than replacing cation from the synthesis viewpoint [50,51].

3.3.2. The structure–reactivity relationship of IC- and NIC-catalysts

To predict the reactivity of catalyst based on its structure is the aim of catalyst design. Each catalyst investigated in this manuscript has its unique performance. Based on above investigation, some relationships can be established between reactivity and SD, Q, or IFCC parameters.

(1) Relationship between the SD and reactivity: The reaction barriers were used as *y*-axis, and the SD values carried by Fe and O were used as *x*-axis, respectively (Fig. 8). A linear or almost linear relation can be found between the SD_{Fe} (or SD_O) and the reactivity. The correlation coefficients are 0.925 and 0.945 for SD_{Fe} and SD_O, respectively.

$$\text{Barrier} = 197.59SD_{Fe} - 147.12 \quad (R^2 = 0.925)$$
$$\text{Barrier} = -202.07SD_O + 255.16 \quad (R^2 = 0.945)$$

Designing more powerful catalyst becomes much easier with these formulas. The presented calculated results suggest that modification that leads to smaller SD_{Fe} and larger SD_O will give a more powerful catalyst. It has been found that $(N_4Py)Fe{=}O$ is more reactive than Compound I of P450 [47]. It is interesting to find that the SD_{Fe} value of the LSS $(N_4Py)Fe{=}O$ is 1.06, whereas the same value of the LSS Compound I of P450 is 1.17. At the same time, the SD_O value of the LSS $(N_4Py)Fe{=}O$ is 0.98, whereas the same value of the LSS Compound I of P450 is 0.92 [34,37,47].

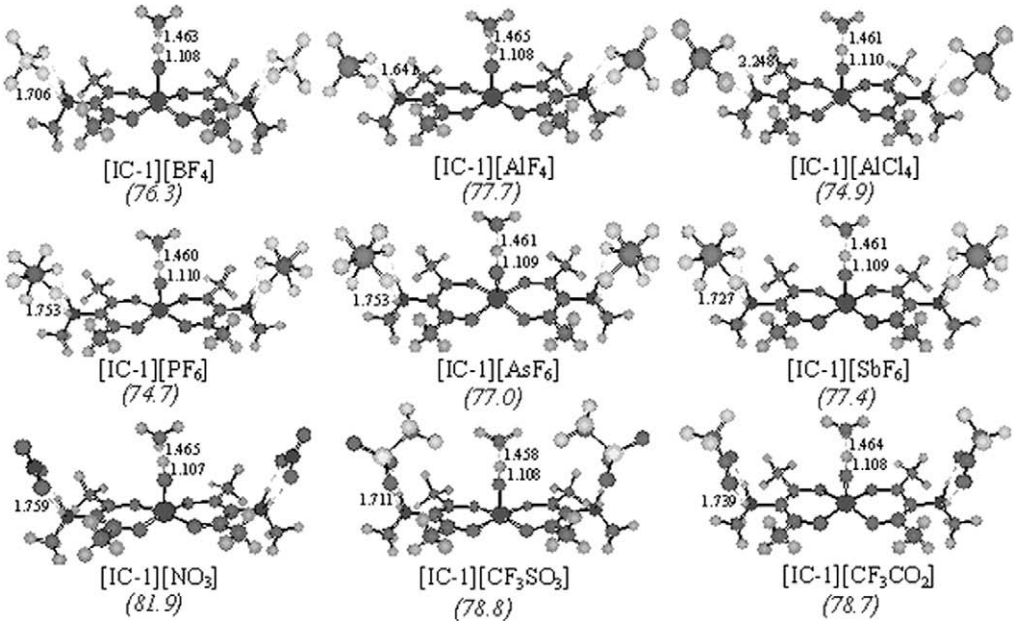

Fig. 7. The optimized transition states catalyzed by IC-catalyst with different anions. The values in parenthesis mean reaction barrier in kJ/mol. The other values denote bond lengths in Å.

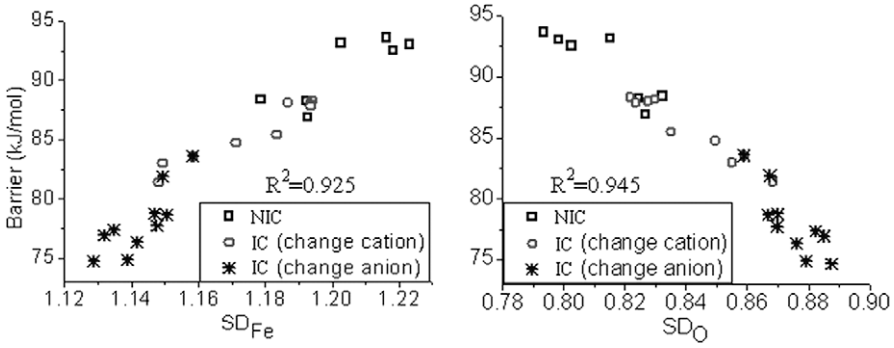

Fig. 8. The relationships between the reaction barriers and the SD_{Fe}/SD_O values.

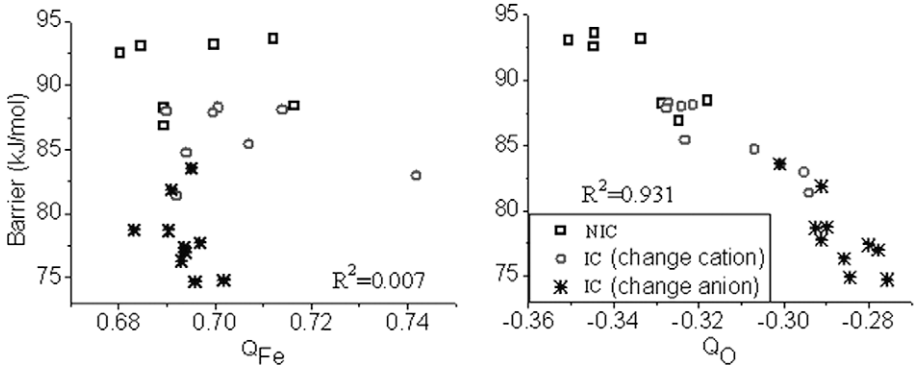

Fig. 9. The relationships between the reaction barriers and the Q_{Fe}/Q_O values.

(2) Relationship between the Q and reactivity: The reaction barriers were used as *y*-axis, and the Q values carried by Fe and O were used as *x*-axis, respectively (Fig. 9). No linear relation can be found between the Q_{Fe} and the reactivity. However, the Q_O shows an almost linear relation with the reactivity of the catalyst.

$$\text{Barrier} = -253.35Q_O + 5.85 \quad (R^2 = 0.931)$$

This suggests that the less negative charge the O atom carries, the more powerful the catalyst is.

(3) Relationship between the IFCC and reactivity: The IFCC relates to the hyperfine splitting constant of the corresponding EPR spectrogram, which is a useful property for understanding the structure of compound with unpaired electron. An almost linear relation can also be found between the $IFCC_O$ and the reactivity (Fig. 10).

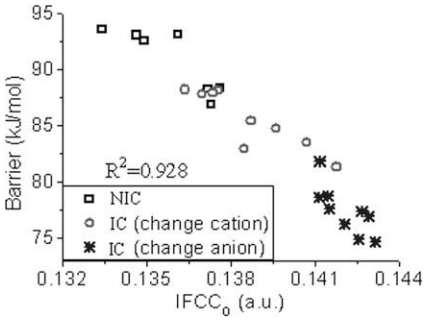

Fig. 10. The relationship between the reaction barriers and the IFCC$_O$.

$$\text{Barrier} = -2025.7\text{IFCC}_O + 365.9 \quad (R^2 = 0.928)$$

That is, modification that leads to larger IFCC$_O$ gives a more powerful catalyst.

(4) Relationship between the HOMO–LUMO gap and reactivity: Previously, the HOMO–LUMO gap is usually used to predict the reactivity of catalysts [52–54]. Two kinds of HOMO–LUMO gaps were investigated here: the HOMO–LUMO gap of the catalyst (Fig. 11) and the HOMO–LUMO gap between the catalyst and reactant (Fig. 12).

Based on the analysis on a lot of different catalysts, it was found that the HOMO–LUMO gap of the catalyst was not correlative with the reactivity (Fig. 11). This result does not agree with some previous researches which suggested smaller HOMO–LUMO gap of the catalyst leading to higher reactivity. This relativity may be occasional because only three or four catalysts were tested [41,54]. Indeed, the HOMO–LUMO gap of the catalyst describes the ability of the electron transfer from the HOMO to the LUMO. This value is a little meaningful for the reactivity when electron transfers from the catalyst to the reactant. For the C–H activation investigated here, the electron transfer from the reactant to the catalyst during the reaction.

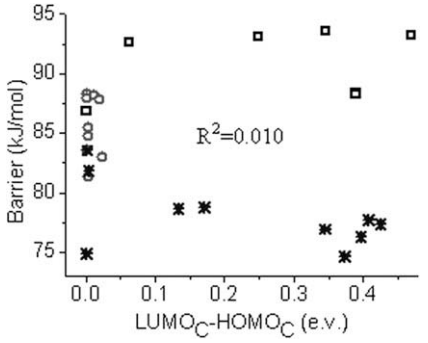

Fig. 11. The relationship between the reaction barriers and the HOMO–LUMO gap of the catalysts.

Frontier molecular orbital theory has received great success in the prediction of reactivity [52]. The HOMO–LUMO gaps between the catalyst and reactant were carefully investigated, and these gaps were correlated with their reactivity (Fig. 12). It was found that there existed a relativity to some extent. But the correlation is quite low (only 0.637). By comparing the structures of the reactant and transition state, we found that the structure distortions were quite obvious for the reaction catalyzed by IC-catalysts with different cations. As we know, the structure distortion itself can induce energy change [55]. The structure distortion is relative to the steric interaction, and it is difficult to be predicted from the catalyst structure itself. If the values of IC-catalysts with different cation are excluded, the correlation coefficient increases from 0.637 to 0.883.

The following structural parameters have been correlated with the reactivity of the catalysts: SD$_{Fe}$, SD$_O$, Q_{Fe}, Q_O, IFCC$_O$, LUMO$_C$–HOMO$_C$, and LUMO$_C$–HOMO$_R$. The order of the correlation coefficient is: R^2 (SD$_O$) > R^2 (QQ_O) > R^2 (IFCC$_O$) ≈ R^2 (SD$_{Fe}$) > 0.9 > R^2 (LUMO$_C$–HOMO$_R$) ≫ R^2 (LUMO$_C$–HOMO$_C$) ≈ R^2 (Q_{Fe}) ≈ 0.

3.4. The structure–reactivity relationship of different spin state IC- and NIC-catalysts

Transition metal catalysts are known to have low- and high-spin state [41], both of which were taken into consideration in this study. Because the LSS reaction pathway is more energy favorable, only parts of the HSS catalysts were further investigated. These HSS catalysts include the most powerful catalyst ([IC-1][PF$_6$]), the catalyst with the lowest reactivity (NIC-3), the unmodified catalyst NIC-1, and some other five representative catalysts (Table 4).

As shown in Table 4, the structure parameters of the Fe=O active center of HSS catalysts are obviously different from those of the LSS catalysts. The HSS catalysts carry two more isolated electrons, and the calculated results suggest that these two electrons distribute mainly in the Fe atom. The following values of LSS catalysts are larger than those of HSS catalysts: Fe–O bond length, SD$_O$, and IFCC$_O$. The following values of LSS catalysts are smaller than those of HSS catalysts: SD$_{Fe}$ and Q_{Fe}. There exist some intersections for the Q_O and HOMO–LUMO gap of LSS and HSS catalysts. These differences determine that the reactivity of HSS catalysts will be quite different from that of the LSS catalysts. The obtained results of reactivity indicate that the LSS catalysts are more powerful than their corresponding HSS catalysts (Fig. 13).

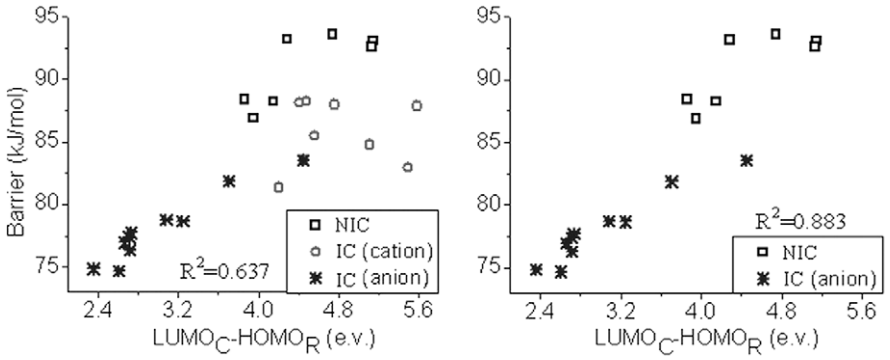

Fig. 12. The relationship between the reaction barriers and the HOMO–LUMO gap of the catalyst-reactant. The subscript C means catalyst and R means reactant.

Table 4
Structure parameters of different catalysts (LSS and HSS) with axial ligand.

	r(Fe–O)[a]	SD_{Fe}	SD_O	Q_{Fe}	Q_O	Q_{anion}[b]	$IFCC_O$ (a.u.)	Gap[c]
LSS								
[IC-1][Cl]-py	1.660	1.018	1.036	0.515	−0.271	−0.597	0.1681	0.0001
[IC-2][Cl]-py	1.660	1.008	1.043	0.513	−0.265	−0.547	0.1690	0.0021
[IC-5][Cl]-py	1.658	1.053	1.004	0.524	−0.289	−0.601	0.1637	0.0008
[IC-1][CF_3CO_2]-py	1.661	1.006	1.051	0.507	−0.257	−0.719	0.1697	0.1399
[IC-1][PF_6]-py	1.661	0.988	1.071	0.506	−0.244	−0.793	0.1720	0.1927
NIC-1-py	1.658	1.062	0.995	0.526	−0.295		0.1632	0.1952
NIC-2-py	1.658	1.076	0.978	0.511	−0.307		0.1612	0.1995
NIC-3-py	1.655	1.068	0.978	0.539	−0.303		0.1610	0.1526
HSS								
[IC-1][Cl]-py	1.650	2.979	0.739	0.690	−0.299	−0.599	0.1469	0.0407
[IC-2][Cl]-py	1.649	2.976	0.744	0.688	−0.291	−0.550	0.1476	0.0387
[IC-5][Cl]-py	1.651	3.003	0.702	0.695	−0.324	−0.602	0.1423	0.0085
[IC-1][CF_3CO_2]-py	1.650	2.981	0.743	0.687	−0.293	−0.720	0.1473	0.0159
[IC-1][PF_6]-py	1.650	2.974	0.760	0.689	−0.280	−0.794	0.1494	0.1739
NIC-1-py	1.650	3.009	0.699	0.699	−0.322		0.1420	0.1443
NIC-2-py	1.651	3.015	0.682	0.680	−0.336		0.1400	0.5472
NIC-3-py	1.651	3.030	0.693	0.705	−0.331		0.1415	0.1853

[a] Distance between Fe and O (in Å).
[b] The charge carried by anion.
[c] The HOMO–LUMO gap of the catalyst (in eV).

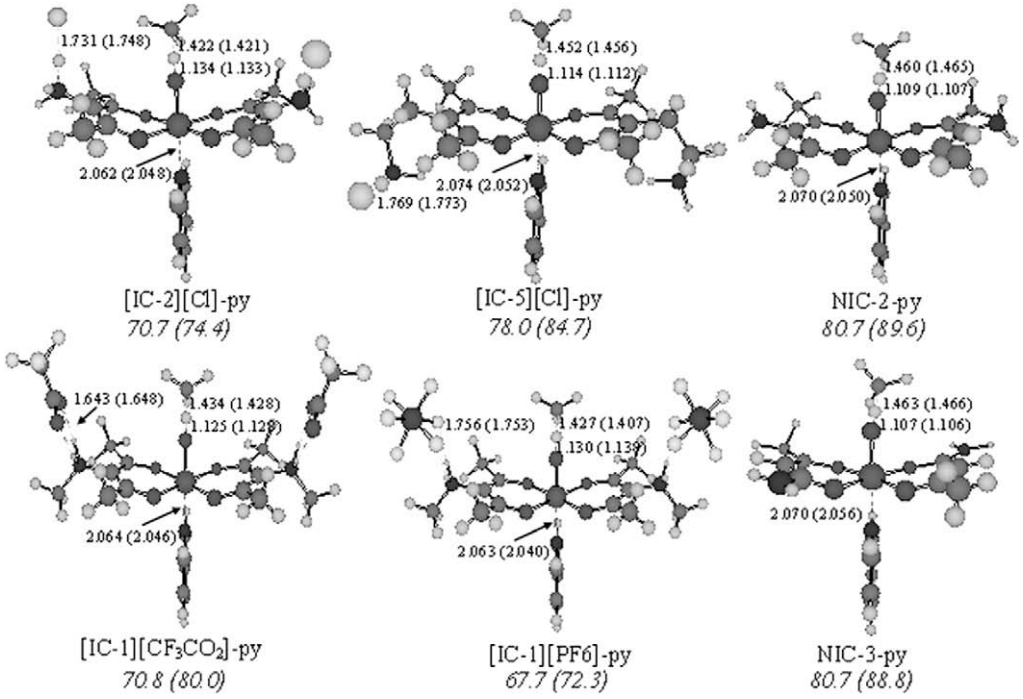

Fig. 13. The optimized transition states catalyzed by IC- and NIC-catalyst with axial ligand. The italic values mean reaction barrier in kJ/mol. The other values denote bond lengths in Å. Values out (in) parentheses are those for the LSS (HSS).

In Section 3.3, the structure–reactivity relationships of IC- and NIC-catalysts without axial ligand have been summarized. In this part, the axial ligand was taken into consideration for both LSS and HSS catalysts. There still exists linear or almost linear relation between the $SD_{Fe}/SD_O/Q_O/IFCC_O$ values and the reactivity of different spin state catalysts with axial ligand (Fig. 14). Modification that increases the SD_O, Q_O, and $IFCC_O$ or decreases SD_{Fe} gives a more powerful catalyst.

For part of structure parameters, there exists systemic difference. Taking the SD_O value as example, there is an order for the SD_O values: SD_O of LSS catalyst with axial ligand >SD_O of LSS catalyst without axial ligand >SD_O of HSS catalyst with axial ligand (Fig. 15). Hence, it is hard to correlate the SD_O values of all the catalysts with their reactivities. In this case, the SD_O value can only be used to predict the reactivity of analogous catalysts. That is, the SD_O–reactivity relationship of LSS catalysts can be used to predict the reactivity of other LSS catalysts but not HSS catalysts. However, there still exist some structure parameters which can be used to predict the reactivity of different kind catalysts. Taking the Q_O value as example, the SD_O values of all the catalysts (LSS, HSS catalysts with and without axial ligand) are correlative with their reactivities. The correlation coefficients are 0.919.

$$\text{Barrier} = -260.74Q_O + 2.96 \quad (R^2 = 0.919)$$

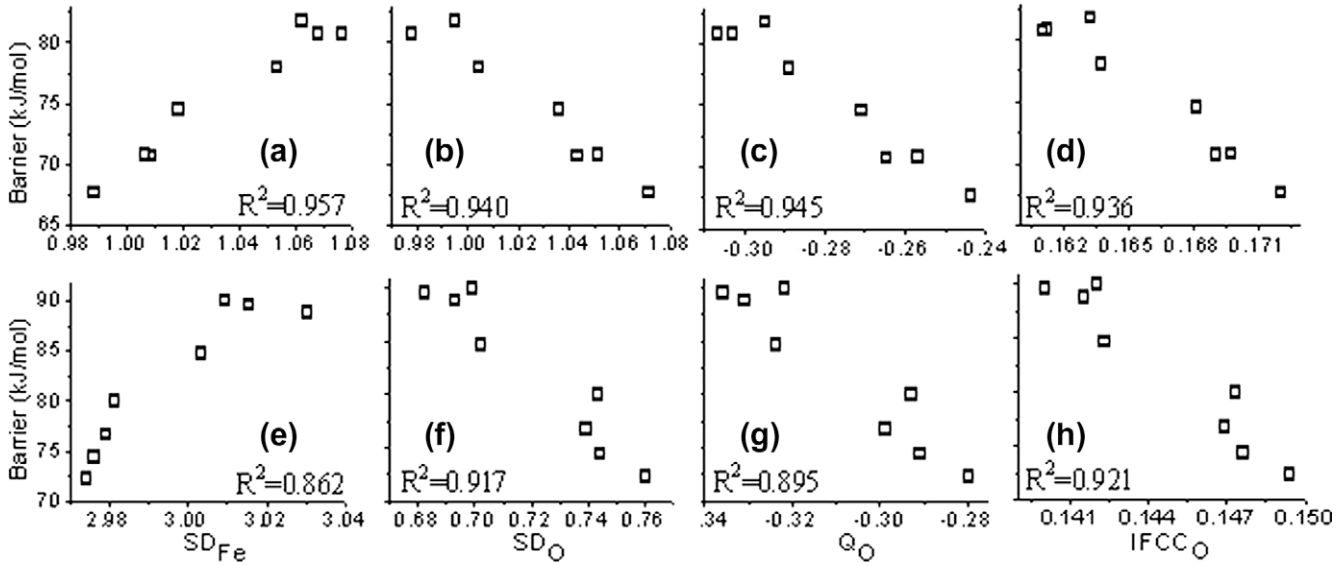

Fig. 14. The relationships between the reaction barriers and $SD_{Fe}/SD_O/Q_O/IFCC_O$ of catalysts with axial ligand. (a–d) LSS catalyst; (e–f) HSS catalyst.

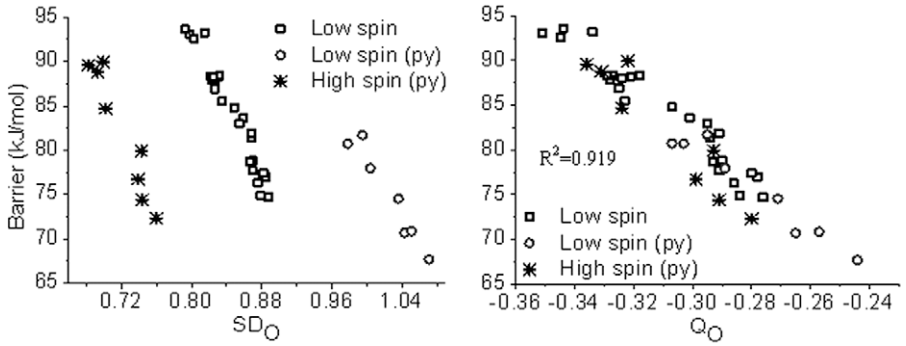

Fig. 15. The relationships between the reaction barriers and SD_O/Q_O of all catalysts. Py means catalysts with pyridine as axial ligand.

For different catalysts (LSS, HSS catalysts with and without axial ligand), this Q_O–reactivity relationship is uniform. The less negative charge the O atom carries, the more powerful the catalyst is.

3.5. Results obtained by alternative calculation methods

Alternative calculation methods were applied to confirm the obtained results. These methods include (1) using different basis sets (CEP-121G or LANL2DZ for Fe and 6-31G*, 6-311 + G*, or 6-311++G** for other atoms) to optimize the structure and (2) taking the effects of environment into consideration. Because of the heavy computational works, only parts of the catalysts were recalculated.

Table 5
Structure parameters and C–H activation barriers (in kJ/mol) calculated by different methods.

Basis set	Catalyst	SD_{Fe}	SD_O	Q_{Fe}	Barrier
B[a]	NIC-1-py	1.200	0.862	−0.436	90.4
	[IC-1][Cl]-py	1.160	0.900	−0.409	87.0
C[b]	NIC-1-py	1.125	0.902	−0.230	88.2
	[IC-1][Cl]-py	1.053	0.942	−0.215	83.3
D[c]	NIC-1-py	1.194	0.939	−0.233	93.3
	[IC-1][Cl]-py	1.179	0.970	−0.196	87.7
E[d]	NIC-1-py	1.112	0.904	−0.219	94.3
	[IC-1][Cl]-py	1.077	0.939	−0.196	88.8

[a] Optimized using basis set B.
[b] Optimized using basis set C.
[c] Optimized using basis set D.
[d] Optimized using basis set E.

Table 6
Structure parameters and C–H activation barriers (in kJ/mol) in environments with different dielectric constants (ε).[a]

Catalyst	SD_{Fe}	SD_O	Q_{Fe}	Q_O	$IFCC_O$	Barrier
ε = 1.0						
NIC-1-py	1.062	0.995	0.526	−0.295	0.1632	100.5
[IC-1][Cl]-py	1.019	1.036	0.515	−0.271	0.1681	92.7
ε = 4.9						
NIC-1-py	1.172	0.901	0.510	−0.338	0.1431	99.6
[IC-1][Cl]-py	1.127	0.943	0.507	−0.315	0.1477	92.4
ε = 8.9						
NIC-1-py	1.179	0.894	0.509	−0.345	0.1423	99.0
[IC-1][Cl]-py	1.135	0.936	0.507	−0.322	0.1471	93.5
ε = 20.7						
NIC-1-py	1.184	0.890	0.508	−0.349	0.1419	99.0
[IC-1][Cl]-py	1.139	0.933	0.507	−0.326	0.1467	92.9
ε = 36.6						
NIC-1-py	1.186	0.888	0.507	−0.350	0.1416	98.5
[IC-1][Cl]-py	1.142	0.930	0.506	−0.328	0.1465	92.6
ε = 78.4						
NIC-1-py	1.229	0.849	0.491	−0.381	0.1370	98.2
[IC-1][Cl]-py	1.183	0.893	0.491	−0.357	0.1418	93.3

[a] Energies listed here are total electronic energy.

The results obtained with other basis sets confirm that the [IC-1][Cl]-py is more reactive than the NIC-1-py catalyst (Table 5). Corresponding to the reactivity, the following relation still works: SD_{Fe} of NIC-1-py > SD_{Fe} [IC-1][Cl]-py, SD_O of NIC-1-py < SD_O [IC-1][Cl]-py, Q_O of NIC-1-py < Q_O [IC-1][Cl]-py.

Since the IC-modified catalysts were generally used in different kind of solvents (e.g. $CHCl_3$, CH_3CN, and H_2O) [3–4], we further performed our research in the environments with different polarities (ε = 4.9, 8.9, 20.7, 36.6, and 78.4) (Table 6). These results also confirm the main results obtained above. That is, modification that increases the SD_O, Q_O, and $IFCC_O$ or decreases SD_{Fe} value makes the catalyst more powerful.

4. Conclusions

The structures and reactivities of 41 different IC- and NIC-catalysts were investigated. The cations of the IC-catalysts include ammonium, pyridinium, and imidazolium salts, and the anions include BF_4^-, PF_6^-, SbF_6^-, AsF_6^-, $CF_3SO_3^-$, $CF_3CO_2^-$, NO_3^-, AlF_4^-, $AlCl_4^-$, and Cl^-. The following structure parameters were carefully investigated: SD_{Fe}, SD_O, Q_{Fe}, Q_O, $IFCC_O$, $LUMO_C$–$HOMO_C$, and $LUMO_C$–$HOMO_R$. These structure parameters were correlated with the reactivity of the catalysts.

Based on the results obtained from our investigations, the following can be safely stated: (a) The IC-modification can influence all of the following parameters: SD_{Fe}, SD_O, Q_{Fe}, Q_O, $IFCC_O$, and $LUMO_C$–$HOMO_C$. The SD_{Fe}, SD_O, Q_O, and $IFCC_O$ have an almost linear relation with the reactivity for the analogous catalysts. Their correlations are even stronger than that of the $LUMO_C$–$HOMO_R$ gap. The order of the correlation coefficient is: R^2 (SD_O) > R^2 (Q_O) > R^2 (SD_{Fe}) ≈ R^2 ($IFCC_O$) > 0.9 > R^2 ($LUMO_C$–$HOMO_R$) ≫ R^2 ($LUMO_C$–$HOMO_C$) ≈ R^2 (Q_{Fe}) ≈ 0. Modification that increases the SD_O, Q_O, and $IFCC_O$ or decreases SD_{Fe} gives a more powerful catalyst. The Q_O–reactivity relationship works without the limitation of the kind of catalysts. (b) Changing the anion is more effective way to increase the reactivity of the IC-catalyst compared with changing the cation. For the anions, the order of the ability to affect the reactivity is: $PF_6^- > AlCl_4^- > BF_4^- > AsF_6^- > SbF_6^- > AlF_4^- > CF_3CO_2^- > CF_3SO_3^- > NO_3^- > Cl^-$. For the cations, the ammonium salt is more powerful to alter the reactivity than pyridinium and imidazolium salts. (c) Most of the IC-modification methods can increase the reactivity of the catalysts. Long distance between the IC part and the catalytic active center can weaken the influence induced by IC-modification.

While we presented the structural cause underlying the reactivity-enhancing effects of the IC-modification, we realize that this is unlikely to be the sole cause. We believe that IC-modification could influence reactions in two different ways. The first way, relatively well studied [1,50,51], is promoting catalyst diffusion. Ionic salt is capable of bringing inorganic and organic reagents/catalysts into the same phase, which promotes reactions. The other way is influencing the reaction process itself, and the case presented herein is an example.

Most of the previous experiments suggested that the IC-immobilization increased the reaction rate [7,18–24]. However, there are also experimental data showing that this immobilization weakened the reactivity of the catalyst [9]. The presented theoretic and our previous experimental [24] study gives an example of how to improve the reactivity of the catalyst by IC-modification method. We also believe that some other modification methods can lower the catalytic ability of the catalyst. The roles (improving or weakening) of the modification on the reactivity of the catalyst should depend on the modification position and the combination between the anion and cation. As we know, the current IC-modification methods reported in references are mainly used for the purpose of making the catalyst reusable [3–24]. The structure–reactivity relationships summarized here are expected to be used in designing a more powerful catalyst.

Acknowledgment

This work was supported by the National Natural Science Foundation of China (Nos. 20990221, 20773109, and 20803062).

Appendix A. Supplementary material

Supplementary data associated with this article can be found, in the online version, at doi:10.1016/j.jcat.2010.04.016.

References

[1] Q.H. Fan, Y.M. Li, A.S.C. Chan, Chem. Rev. 102 (2002) 3385.
[2] M. Hatano, T. Maki, K. Moriyama, M. Arinobe, K. Ishihara, J. Am. Chem. Soc. 130 (2008) 16858.
[3] W.S. Miao, T.H. Chan, Acc. Chem. Res. 39 (2006) 897.
[4] R. Sebesta, I. Kmentova, S. Toma, Green Chem. 10 (2008) 484.
[5] N. Audic, H. Clavier, M. Mauduit, J.-C. Guillemin, J. Am. Chem. Soc. 125 (2003) 9248.
[6] Q. Yao, Y. Zhang, Angew. Chem., Int. Ed. 42 (2003) 3395.
[7] R. Tan, D.H. Yin, N.Y. Yu, Y. Jin, H. Zhao, D. Yin, J. Catal. 255 (2008) 287.
[8] M. Lombardo, M. Chiarucci, C. Trombini, Green Chem. 11 (2009) 574.
[9] T.J. Geldbach, P.J. Dyson, J. Am. Chem. Soc. 126 (2004) 8114.
[10] A.C. Pinto, A.A.M. Lapis, B.V. Da Silva, R.S. Bastos, J. Dupont, B.A.D. Neto, Tetrahedron Lett. 49 (2008) 5639.
[11] D.B. Zhao, Z. Fei, T.J. Geldbach, R. Scopelliti, P.J. Dyson, J. Am. Chem. Soc. 126 (2004) 15876.
[12] K. Yamaguchi, C. Yoshida, S. Uchida, N. Mizuno, J. Am. Chem. Soc. 127 (2005) 530.
[13] A.C. Cole, J.L. Jensen, I. Ntai, K.L.T. Tran, K.J. Weaver, D.C. Forbes, J.H. Davis Jr., J. Am. Chem. Soc. 124 (2002) 5962.
[14] M. Lombardo, F. Pasi, S. Easwar, C. Trombini, Adv. Synth. Catal. 349 (2007) 2061.
[15] C. Zhong, T. Sasaki, M. Tada, Y. Iwasawa, J. Catal. 242 (2006) 357.
[16] Q. Zhang, B. Ni, A.D. Headley, Tetrahedron 64 (2008) 5091.
[17] M. Lombardo, F. Pasi, S. Easwar, C. Trombini, Synlett 16 (2008) 2471.
[18] C. Baleizao, B. Gigante, H. Garcia, A. Corma, Tetrahedron 60 (2004) 10461.
[19] E.K. Noh, S.J. Na, S. Sujith, S.W. Sang-Wook Kim, B.Y. Lee, J. Am. Chem. Soc. 129 (2007) 8082.
[20] W.S. Miao, T.H. Chan, Adv. Synth. Catal. 348 (2006) 1711.
[21] M. Lombardo, S. Easwar, F. Pasi, C. Trombini, Adv. Synth. Catal. 351 (2009) 276.
[22] R. Tan, D.H. Yin, N.Y. Yu, Y. Jin, H. Zhao, D. Yin, J. Catal. 263 (2009) 284.
[23] M.D. Nguyen, L.V. Nguyen, E.H. Jeon, J.H. Kim, M. Cheong, H.S. Kim, J.S. Lee, J. Catal. 258 (2008) 5.
[24] X.B. Hu, J.Y. Mao, Y. Sun, H. Chen, H.R. Li, Catal. Commun. 10 (2009) 1908.
[25] B.L. Bhargava, S. Balasubramanian, J. Am. Chem. Soc. 128 (2006) 10073.
[26] R.M. Lynden-Bell, M.G.D. Popolo, T.G.A. Youngs, J. Kohanoff, C.G. Hanke, J.B. Harper, C.C. Pinilla, Acc. Chem. Res. 40 (2007) 1138.
[27] A.A.H. Padua, M.F. Costa Gomes, J.N. Canongia Lopes, Acc. Chem. Res. 40 (2007) 1087.
[28] C.S. Pomelli, C. Chiappe, A. Vidis, G. Laurenczy, P.J. Dyson, J. Phys. Chem. B 111 (2007) 13014.
[29] K. Mylvaganam, G.B. Bacskay, N.S. Hush, J. Am. Chem. Soc. 122 (2000) 2041.
[30] C. Jones, D. Taube, V.R. Ziatdinov, R.A. Periana, R.J. Nielsen, J. Oxgaard, W.A. Goddard III, Angew. Chem., Int. Ed. 43 (2004) 4626.
[31] D.K. Bōhme, H. Schwarz, Angew. Chem., Int. Ed. 44 (2005) 2336.
[32] S. Feyel, J. Dōbler, D. Schröder, J. Sauer, H. Schwarz, Angew. Chem., Int. Ed. 45 (2006) 4681.
[33] X.B. Hu, H.R. Li, C.M. Wang, J. Phys. Chem. B 110 (2006) 14046.
[34] X.B. Hu, H.R. Li, J. Phys. Chem. A 111 (2007) 8352.
[35] M.H. Baik, M. Newcomb, R.A. Friesner, S.J. Lippard, Chem. Rev. 103 (2003) 2385.
[36] S. Shaik, D. Kumar, S.P. de Visser, A. Altun, W. Thiel, Chem. Rev. 105 (2005) 2279.
[37] F. Ogliaro, N. Harris, S. Cohen, M. Filatov, S.P. de Visser, S. Shaik, J. Am. Chem. Soc. 122 (2000) 8977.
[38] A. Altun, S. Shaik, W. Thiel, J. Am. Chem. Soc. 129 (2007) 8978.
[39] X.B. Hu, C.M. Wang, Y. Sun, H. Sun, H.R. Li, J. Phys. Chem. B 112 (2008) 10684.
[40] S.P. de Visser, J. Am. Chem. Soc. 132 (2010), doi:10.1021/ja908340j.
[41] D. Schröder, S. Shaik, H. Schwarz, Acc. Chem. Res. 33 (2004) 139.
[42] M.J. Frisch, G.W. Trucks, H.B. Schlegel, G.E. Scuseria, M.A. Robb, J.R. Cheeseman, V.G. Zakrzewski, J.A. Montgomery, Jr., R.E. Stratmann, J.C. Burant, S. Dapprich, J.M. Millam, A.D. Daniels, K.N. Kudin, M.C. Strain, O. Farkas, J. Tomasi, V. Barone, M. Cossi, R. Cammi, B. Mennucci, C. Pomelli, C. Adamo, S. Clifford, J. Ochterski, G.A. Petersson, P.Y. Ayala, Q. Cui, K. Morokuma, D.K. Malick, A.D. Rabuck, K. Raghavachari, J.B. Foresman, J. Cioslowski, J.V. Ortiz, A.G. Baboul, B.B. Stefanov, G. Liu, A. Liashenko, P. Piskorz, I. Komaromi, R. Gomperts, R.L.

Martin, D.J. Fox, T. Keith, M.A. Al-Laham, C.Y. Peng, A. Nanayakkara, M. Challacombe, P.M.W. Gill, B. Johnson, W. Chen, M.W. Wong, J.L. Andres, C. Gonzalez, M. Head-Gordon, E.S. Replogle, J.A. Pople, GAUSSIAN 03, Gaussian, Inc., Pittsburgh, PA, 2003.
[43] Y. Ishii, S. Sakaguchi, T. Iwahama, Adv. Synth. Catal. 343 (2001) 395.
[44] T. Iwahama, Y. Yoshino, T. Keitoku, S. Sakaguchi, Y. Ishii, J. Org. Chem. 65 (2000) 6502.
[45] A. Lattanzi, A. Senatore, A. Massa, A. Scettri, J. Org. Chem. 68 (2003) 3691.
[46] D. Kumar, E. Derat, A.M. Khenkin, R. Neumann, S. Shaik, J. Am. Chem. Soc. 127 (2005) 17712.
[47] D. Kumar, H. Hirao, L.Q. Jr, S. Shaik, J. Am. Chem. Soc. 127 (2005) 8026.
[48] S.P. Smidt, N. Zimmermann, M. Studer, A. Pfaltz, Chem. Eur. J. 10 (2004) 4685.
[49] C. Moreau, C. Hague, A.S. Weller, C.G. Frost, Tetrahedron Lett. 42 (2001) 6957.
[50] T. Welton, Chem. Rev. 99 (1999) 2071.
[51] J. Dupont, R.F. de Souza, P.A.Z. Suarez, Chem. Rev. 102 (2002) 3667.
[52] K. Fukui, T. Yonezawa, H. Shingu, J. Chem. Phys. 20 (1952) 722.
[53] R.B. De Vasher, J.M. Spruell, D.A. Dixon, G.A. Broker, S.T. Griffin, R.D. Rogers, K.H. Shaughnessy, Organometallics 24 (2005) 962.
[54] C. Tabares-Mendoza, P. Guadarrama, J. Organomet. Chem. 691 (2006) 2978.
[55] D.H. Ess, K.N. Houk, J. Am. Chem. Soc. 130 (2008) 10187.